The rolling motion of an eccentrically loaded wheel

W. F. D. Theron

Citation: American Journal of Physics **68**, 812 (2000); doi: 10.1119/1.1302324
View online: http://dx.doi.org/10.1119/1.1302324
View Table of Contents: http://scitation.aip.org/content/aapt/journal/ajp/68/9?ver=pdfcov
Published by the American Association of Physics Teachers

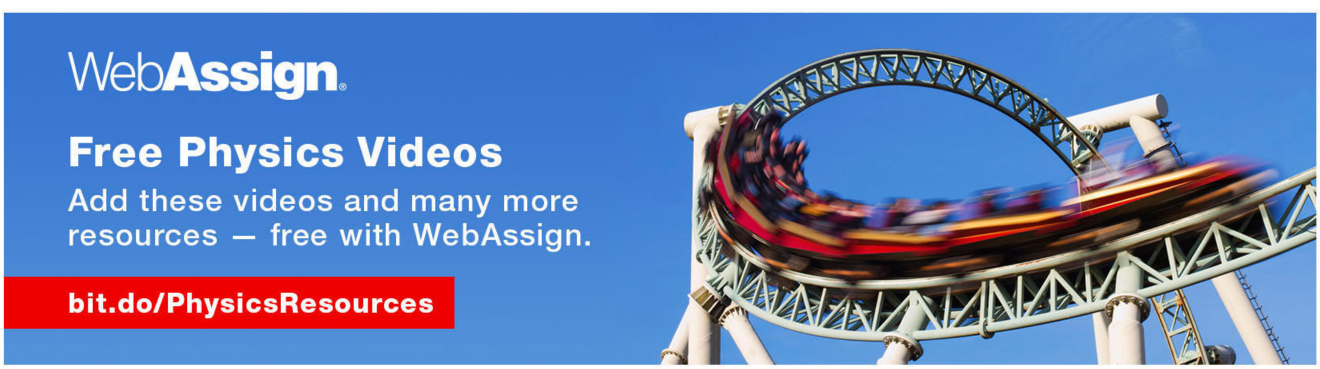

The rolling motion of an eccentrically loaded wheel

W. F. D. Theron[a)]
Department of Applied Mathematics, University of Stellenbosch, Private Bag X1, Matieland, 7602, South Africa

(Received 5 March 1999; accepted 16 December 1999)

This article discusses the rolling motion on a rough plane of a wheel whose center of mass does not coincide with the axis; for example, when a heavy particle is fixed to the rim of a rigid hoop. In cases with large eccentricity, the resulting motion is surprisingly complex, with four phases being identified, namely rolling (without slipping), spinning, skidding, and ''hopping,'' by which is meant that the wheel actually leaves the plane. The main result of this analysis is the identification of the conditions that are required for hopping to occur. A second result is that faster than gravity accelerations occur when the mass of the particle is greater than the mass of the hoop. Massless hoops are briefly discussed as a special case of the general results.

I. INTRODUCTION

The phenomenon of the ''hopping hoop'' has received some attention recently,[1,2] many years after first being published in 1953 in *A Mathematician's Miscellany* by J. E. Littlewood. The following formulation and ''solution'' is from p. 37 of the recently published revised edition[3] of this book.

> A weight is attached to a point of a rough weightless hoop, which then rolls in a vertical plane, starting near the point of unstable equilibrium. What happens, and is it intuitive?
>
> The hoop lifts off the ground when the radius vector to the weight becomes horizontal. I don't find the lift directly intuitive; one can however ''see'' that the motion is equivalent to the weight's sliding smoothly under gravity on the cycloid it describes, and it is intuitive that it will sooner or later leave that. (But the ''seeing'' involves the observation that *P* is instantaneously rotating about *C* (Fig. 1).)
>
> Mr. H. A. Webb sets the question annually to his engineering pupils, but I don't find it in books.
>
> In actual practice the hoop skids first.

This is all that Littlewood says about the problem in this book. His remarks seem to have been accepted (or unnoticed!) for more than 40 years, until 1997 when Tokieda[1] published an ingenious analysis based on the fact that the path of the particle changes from a cycloid to a parabola. He interpreted this as supporting Littlewood's statement that the hoop lifts off the ground, or *hops*, after rotating through 90°. My intuition refused to accept this, and we[4] have derived equations for an alternative motion in which the massless hoop does not hop but remains in contact with the surface even though the reaction is zero. Butler[2] shows that the hoop cannot hop at this point, but there is a serious error in his proof. This issue will be discussed further in Sec. III H and in a separate paper.[5]

In this paper *real* hoops, in which the mass of the hoop is taken into account, are analyzed. The most general model considered is of an eccentrically loaded wheel, in which the center of mass does not coincide with the axis of rotation. The wheel is given an initial velocity to start it rolling on a rough, possibly sloping, plane. Only rigid wheels are considered, although the elasticity inherent in any real physical model will certainly influence the behavior, somewhat similar to the model in Ref. 6.

The main focus is on cases with very large eccentricities, such as obtained when a heavy particle is fixed to the rim of a light hoop. Hopping can occur in such cases, and the initial conditions which are necessary to cause this are derived and presented as the main result of this analysis. A second interesting feature of such hoops is that they provide another example of a ''faster than gravity'' model (see Ref. 7), in which the acceleration of the hoop can exceed the acceleration due to gravity even though gravity is the only applied force.

A third point of interest is the number of different modes of motion and the large variety of sequences in which they can occur. The following terminology will be used for the different modes (or phases). The wheel is *rolling* when the velocity of the contact point on the wheel relative to the surface is zero. This pure rolling motion ceases when the friction force reaches its maximum value, in which case the wheel starts *slipping*. Two slipping modes can be identified. If the angular velocity is ''too large'' for the forward motion, the wheel is said to be *spinning* and the friction force on the wheel is in the same direction as the forward motion. If the opposite is true, the wheel is said to be *skidding*. Finally, under certain special conditions, the wheel can *hop* (or *bounce*) by leaving the surface.

The analysis is done in terms of forces rather than the energy of the system, because the different phases are identified in terms of the forces. The equations of motion are therefore derived using Newton's second law. Analytic solutions are obtained for the conservative (rolling) phase; in the other phases numerical integration is used to obtain the results given at the end of the paper.

II. THE MATHEMATICAL MODEL

A. Geometry of the wheel

Figure 1 shows a wheel with radius R rolling down a surface which makes an angle φ with the horizontal plane. The total mass of the wheel is M and the center of mass is at point G at a radial distance $r=\gamma R$ from point O, the center of the wheel. Point C is the point of contact and the instantaneous center of rotation.

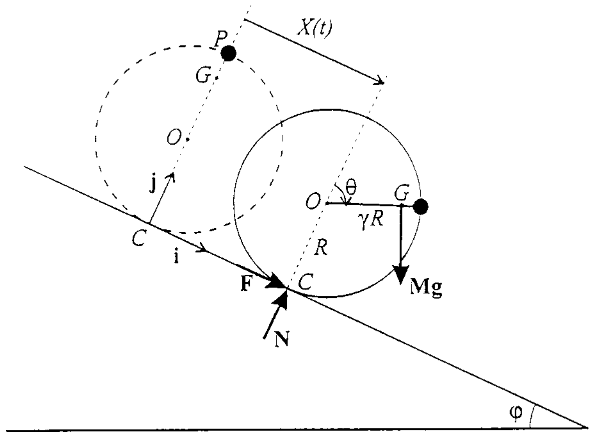

Fig. 1. A loaded wheel; coordinates and forces.

The value of γ is a measure of the eccentricity of the wheel. The cases of interest for the analysis which follows are for large eccentricities, approximately in the range $\gamma \in (0.5;1)$.

The position of the wheel is determined by the angular displacement θ, with the initial position $\theta = 0$ being taken as the position when the radii $C-O-G$ form a straight line.

Moments of inertia will be defined in terms of a factor κ such that the moment of inertia is given by κMR^2. The basic input parameter is the moment of inertia of the wheel about the axis through point O, defined by κ_0 such that $I_O = \kappa_0 MR^2$. By using the parallel axis theorem, the moments of inertia about points G and C, respectively, are then defined by the factors

$$\kappa_G = \kappa_0 - \gamma^2, \quad \kappa_C = \kappa_0 + 1 + 2\gamma \cos\theta. \tag{1}$$

The special case of a *loaded hoop*, consisting of a particle P attached to the rim of a rigid hoop, will be used to illustrate the results. Let m_h denote the mass of the hoop and m the mass of the particle and define the *mass* ratio as $\nu = m_h/m$ so that $M = (1+\nu)m$ and $\gamma = 1/(1+\nu)$. In the *equal mass* case, $m_h = m$, $\nu = 1$, and $\gamma = 0.5$; this will be the heaviest hoop considered in this paper. Also, assuming that $I_{O(\text{hoop})} = m_h R^2$ it follows that $\kappa_0 = 1$, $\kappa_G = (1-\gamma^2)$, and $\kappa_C = 2(1+\gamma\cos\theta)$. Clearly, for $m_h > 0$, $\gamma < 1$ and $\kappa_G > 0$. It is possible to envisage a model with $\gamma > 1$ by placing a heavy particle on a spoke outside the rim of the hoop; however this case is not included in this analysis as it does not raise any new issues.

B. Kinematics

With t denoting time, the coordinates of O are $(X(t), Y(t))$ in a fixed Cartesian coordinate system with axes parallel and perpendicular to the plane as indicated by unit vectors $\mathbf{i}$ and $\mathbf{j}$, and with origin at the contact point in the initial position. The coordinates of the center of mass G are $(x(t), y(t))$ relative to the same axes. Differentiation with respect to t is denoted by an overdot, for example, $\dot{X}$, and differentiation with respect to θ is denoted by a prime, for example, X'. As usual, g denotes the gravitational acceleration.

The wheel has three degrees of freedom, which are here selected as X, Y, and θ. The rigidity of the wheel implies the following constraints for all $t \geq 0$:

$$x(t) = X(t) + \gamma R \sin\theta(t), \quad y(t) = Y(t) + \gamma R \cos\theta(t), \tag{2}$$

and

$$Y(t) \geq R. \tag{3}$$

The inequality is a sufficient criterion for hopping, whereas $Y(t) = R$ defines motion with contact.

One of the fundamental motions of the wheel is *rolling*, characterized by the requirement that contact is maintained and that the contact point C is momentarily at rest; i.e., that $\dot{X} - R\dot{\theta} = 0$, or, using $X(0) = 0$, that $X(t) = R\theta(t)$. Rolling therefore implies the constraints

$$X(t) = R\theta(t), \quad Y(t) = R. \tag{4}$$

The initial position at $t = 0$ is chosen as $\theta(0) = 0$, $X(0) = 0$, and $Y(0) = R$. Denoting the initial angular velocity by $\omega_0 = \dot{\theta}(0)$, and assuming that the motion commences in rolling mode, it follows that the initial velocities have to satisfy $\dot{X}(0) = R\omega_0$ and $\dot{Y}(0) = 0$.

The subsequent modeling is simplified by using nondimensional variables. The nondimensional velocity, centripetal acceleration, and angular acceleration are, respectively, defined as

$$\xi = \dot{X}/\sqrt{gR}, \quad \eta = (R/g)\dot{\theta}^2, \quad \zeta = (R/g)\ddot{\theta}. \tag{5}$$

Note that the definition implies $\eta \geq 0$, $\dot{\eta} = 2\dot{\theta}\zeta$, and $\eta' = 2\zeta$. Also, for rolling motion, $\xi = \sqrt{\eta}$ and $\ddot{X}/g = \zeta$. For these variables we have initial values $\eta(0) = \eta_0 = (R/g)\omega_0^2$ and $\xi(0) = \sqrt{\eta_0}$.

It is convenient for later use to define the *critical initial velocity* $\hat{\eta}_0$ as

$$\hat{\eta}_0 = (1/\gamma)\cos\varphi. \tag{6}$$

Differentiation of (2) with respect to time t gives the nondimensional acceleration components as

$$\begin{aligned} \ddot{x}/g &= \ddot{X}/g + \gamma\zeta\cos\theta - \gamma\eta\sin\theta, \\ \ddot{y}/g &= \ddot{Y}/g - \gamma\zeta\sin\theta - \gamma\eta\cos\theta. \end{aligned} \tag{7}$$

The nondimensional acceleration of the center of gravity is denoted by a, defined as

$$a = (1/g)\sqrt{\ddot{x}^2 + \ddot{y}^2}. \tag{8}$$

C. Kinetics

Figure 1 shows the three forces acting on the wheel while moving in contact with the surface. They are the weight Mg, the normal reaction $N, N \geq 0$, and the friction force F.

Newton's second law determines the relationship between the forces and the accelerations. Taking components in the positive x direction, $Mg\sin\varphi + F = M\ddot{x}$, or, in nondimensional form and using (7),

$$F/Mg = \ddot{X}/g + \gamma\zeta\cos\theta - \gamma\eta\sin\theta - \sin\varphi. \tag{9}$$

Taking components perpendicular to the plane, $N - Mg\cos\varphi = M\ddot{y}$, or, in nondimensional form and using (7) with $\ddot{Y} = 0$,

$$N/Mg = \cos\varphi - \gamma(\zeta\sin\theta + \eta\cos\theta). \tag{10}$$

The maximum value of the friction force places a constraint on the forces. Denoting the coefficient of friction by μ, Coulomb's law states that

$$|F| \leqslant \mu N. \tag{11}$$

Taking clockwise moments about the center of mass, $Nr \sin\theta - F(R + r\cos\theta) = I_G \ddot{\theta}$ or, in nondimensional form and using (1) and (5),

$$\kappa_G \zeta = (N/Mg)\gamma \sin\theta - (F/Mg)(1 + \gamma\cos\theta). \tag{12}$$

D. Rolling

If the wheel is rolling, $\ddot{X} = R\ddot{\theta}$ from (4), and (9) becomes

$$F/Mg = (1 + \gamma\cos\theta)\zeta - \gamma\eta \sin\theta - \sin\varphi. \tag{13}$$

Substituting this and (10) in (12), rearranging and using (1) results in

$$\kappa_c \zeta = \gamma\eta\sin\theta + \gamma\sin(\theta + \varphi) + \sin\varphi. \tag{14}$$

Using $\eta' = 2\zeta$, this can be written as a linear first-order differential equation in η which can be integrated with respect to θ to give the analytic solution

$$\eta = \frac{2}{\kappa_c}(-\gamma\cos(\theta + \varphi) + \theta\sin\varphi + C). \tag{15}$$

The integration constant C is found from the conditions at the point where rolling starts. Initially this is at the point $\theta = 0$, where $C = C_0$ is used, with

$$C_0 = 0.5\eta_0(\kappa_0 + 1 + 2\gamma) + \gamma\cos\varphi.$$

As shown later, the rolling motion can resume at position θ_3 where $\eta(\theta_3) = \eta_3$, in which case

$$C = 0.5\eta_3(\kappa_0 + 1 + 2\gamma\cos\theta_3) + \gamma\cos(\theta_3 + \varphi) - \theta_3\sin\varphi.$$

While the friction force is less than the maximum permissible value, Eq. (15) is the solution of η as a function of θ; with this known, (14), (13), and (10) can be used to find ζ, F, and N. If however $|F| = \mu N$ at some stage of the motion, the wheel starts slipping and the solution in Sec. II E must be used.

E. Spinning and skidding

Assume that the wheel rolls until the angular displacement is θ_2 when slipping commences with $N(\theta_2) > 0$ and $|F(\theta_2)| = \mu N(\theta_2)$. The initial conditions for the slipping motion are defined by $\eta_2 = \eta(\theta_2)$ and $\xi_2 = \sqrt{\eta_2}$. The two possibilities for the orientation of the friction force need to be considered separately.

First, the wheel is said to be *spinning* if $R\dot{\theta} > \dot{X}$. In this case the friction force is $\mathbf{F} = +\mu N\mathbf{i}$, and (12) becomes $\kappa_G \zeta = (N/Mg)S(\theta)$, where

$$S(\theta) = \gamma\sin\theta - \mu(1 + \gamma\cos\theta)$$

has been introduced to simplify the notation. Using (10) and solving for ζ gives

$$\zeta = \frac{S(\theta)(\cos\varphi - \gamma\eta\cos\theta)}{\kappa_G + S(\theta)\gamma\sin\theta}. \tag{16}$$

Once again the property $\eta' = 2\zeta$ is used to obtain a differential equation in η:

$$\frac{d\eta}{d\theta} = \frac{2S(\theta)(\cos\varphi - \gamma\eta\cos\theta)}{\kappa_G + S(\theta)\gamma\sin\theta}, \quad \theta > \theta_2, \tag{17}$$

with initial value η_2. No analytical solution could be found and this equation is integrated numerically.

The second possibility is that $R\dot{\theta} < \dot{X}$ with the friction force $\mathbf{F} = -\mu N\mathbf{i}$, in which case the wheel is said to be *skidding*. Then (12) becomes $\kappa_G \zeta = (N/Mg)S(\theta)$ with $S(\theta) = \gamma\sin\theta + \mu(1 + \gamma\cos\theta)$, and (17) can again be used to calculate η numerically.

In both cases, with η known at a specific position, ζ is calculated from (16) and the normal reaction from (10), with (9) now used to calculate the value of $\ddot{X}$. When the wheel is spinning

$$\ddot{X}/g = \sin\varphi - \gamma(\zeta\cos\theta - \eta\sin\theta) + \mu N, \tag{18}$$

and when the wheel is skidding

$$\ddot{X}/g = \sin\varphi - \gamma(\zeta\cos\theta - \eta\sin\theta) - \mu N. \tag{19}$$

The appropriate expression for $\ddot{X}$ can be integrated numerically with respect to t to obtain the values of $\dot{X}$.

The motion described by this solution comes to an end in one of the following situations:

(1) at position θ_* where the normal reaction becomes zero; as shown later, the wheel will then bounce in most cases;
(2) at position θ_3 where $\dot{X} = R\dot{\theta}$ when the wheel will start rolling again in most cases—in extreme cases the orientation of the friction force can switch round (spin to skid or vice versa);
(3) at position θ_4 where $\eta(\theta_4) = 0$ and the wheel starts rolling backwards.

F. Hopping

A necessary condition for hopping is that $N = 0$; we denote the values at this point by $N(\theta_*) = 0$ at time t_* with velocity $\eta_* = \eta(t_*)$.

With $N = 0$, the weight acting at the center of mass G is the only force and, from Newton's second law, the components of the acceleration are

$$\ddot{x} = g\sin\varphi, \quad \ddot{y} = -g\cos\varphi, \quad \ddot{\theta} = 0.$$

Clearly, the center of mass G follows a parabolic trajectory and the wheel rotates with a constant angular velocity $\omega_* = \sqrt{(g/R)\eta_*}$. Some of the properties of this parabolic path were derived in Ref. 4 and will not be repeated here.

With $\ddot{y} = -g\cos\varphi$ and $\ddot{\theta} = 0$ in (7) and using (6),

$$\ddot{Y} = g\gamma(\eta\cos\theta - \hat{\eta}_0). \tag{20}$$

The necessary kinematic criterion for hopping of a rigid wheel is clearly that $Y(t) > R$ for $t > t_*$. Because $Y(t_*) = R$ and $\dot{Y}(t_*) = 0$, a sufficient condition for hopping is that $\ddot{Y}_*^+ = \ddot{Y}(t_*^+) > 0$. (Here the notation t_*^+ signifies the value of t immediately following t_*.)

Therefore, from (20), the wheel will hop only if

$$\eta_*\cos\theta_* > \hat{\eta}_0. \tag{21}$$

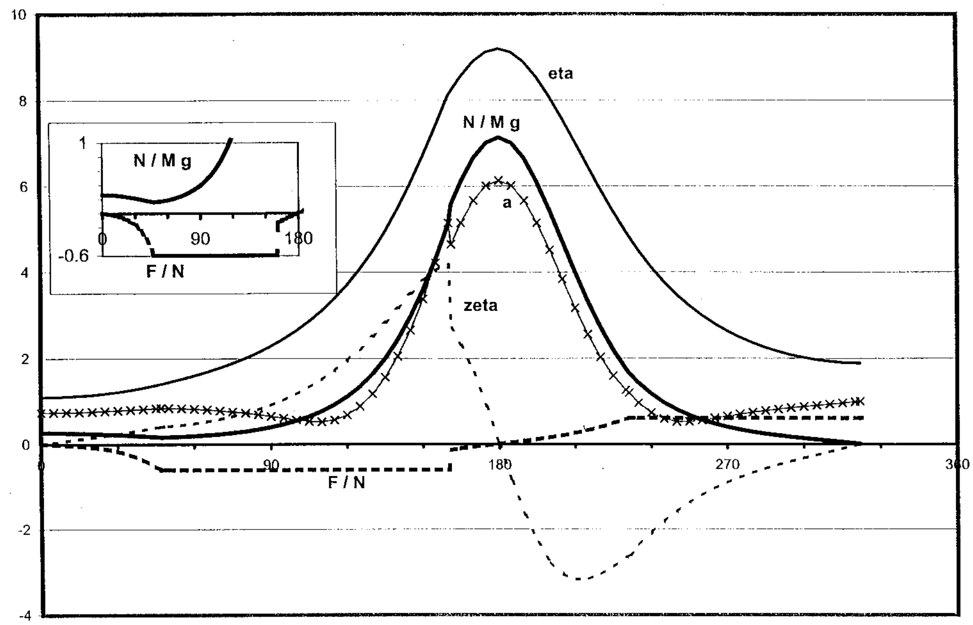

Fig. 2. Variables η, ζ, a, N, F/N as functions of position.

In all examples with real hoops it was found that $\theta_* \in (3\pi/2;2\pi)$ following a slipping phase, so that η_* could only be calculated numerically, and was found to satisfy this criterion for hopping in all cases.

III. RESULTS AND INTERPRETATION

For the rest of this article it will be assumed that $\dot{X}(0) = R\omega_0$ and $\dot{Y}(0)=0$ so that initial rolling occurs, and also that a loaded hoop is being considered, implying that $\kappa_0 = 1$. The dynamic equations of Sec. II now simplify to a four-parameter model in which the behavior depends on the values of the mass ratio ν (which fixes the value of γ), the initial velocity as defined by η_0, the friction coefficient μ, and the slope φ. In the remainder of this section the influence of these parameters on various aspects of the behavior of the hoop are investigated, and it is convenient to define the set of system parameters

$$\mathcal{P}=\{\nu;\eta_0;\mu;\varphi\}$$

for this purpose. In the case of a horizontal plane, the three-parameter problem is defined by

$$\mathcal{P}_0=\{\nu;\eta_0;\mu\}.$$

During the rolling phase (14) and (15) can be substituted in (13) and (10) to obtain the reactions. Once rolling stops due to slipping, further analysis of the various phases of the motion is based on numerical computation. A computer program was developed to do the necessary calculations and create the tables from which the graphs in the following sections could be drawn.

Results for the various examples are presented at two levels. The detailed results for a specific $\mathcal{P}$ are shown as functions of position (θ), where the behavior of the hoop is best seen on the graph of the ratio F/N. Because of the definitions, $F/N=\mu$ indicates a region of spinning, $F/N=-\mu$ indicates skidding, and the regions in between indicate rolling.

The more general behavior is concisely displayed by plotting results on the $\nu-\eta_0$ plane for a given μ and φ.

A. An example of a hopping hoop

As a first example we consider the case $\mathcal{P}_0 = \{0.5;1.1;0.6\}$, especially selected to illustrate most of the interesting characteristics of the loaded hoop. This example is referred to as case c in later discussion; for these values $\gamma=2/3$ and $\hat{\eta}_0=1.5$. The graphs of η, ζ, a, N and F/N are shown in Fig. 2.

Looking at the graphs for N and F/N, it is clear that the hoop rolls initially, with $|F|/N<\mu$ and $F<0$, up to position $\theta_2=46.9°$, where it starts skidding. The skidding motion lasts up to position $\theta_3=160°$; at this point the forces and accelerations change discontinuously and the hoop starts rolling again due to the very large normal reaction in the vicinity of $\theta=180°$. The rolling phase lasts up to 231.3°, where $F=\mu N$ and it starts spinning. Finally, at position $\theta_* = 322.6°$ the normal reaction becomes zero and the hoop hops.

The insert shows that during the first phase of the motion the normal reaction decreases up to position θ_2. At the point where the hoop starts skidding, the normal reaction suddenly starts increasing.

The graph of η displays a peak, with the angular velocity reaching a maximum value of $\sqrt{9.2g/R}$ at position $\theta = 180°$. This large value is due to the very large angular acceleration in the region after $\theta=90°$, reaching a maximum value of $\ddot{\theta}=4.17g/R$ at position $\theta=160°$, where the skidding motion ended. This acceleration becomes smaller as the hoop rolls, is zero at 180°, and then becomes negative as could be expected with the mass moving upwards. At the point where the hoop bounces, the angular velocity is given by $\eta_*=1.890$, so that $\eta_* \cos\theta_*=1.5014$, which exceeds $\hat{\eta}_0=1.5$ as required by (21).

The graph of a also displays a peak, with the interesting aspect that the maximum acceleration of the center of mass is much greater than g; in this case $6.13g$. The loaded hoop is therefore another example of a ''faster than gravity'' model (see Ref. 7), in which the acceleration of the hoop exceeds

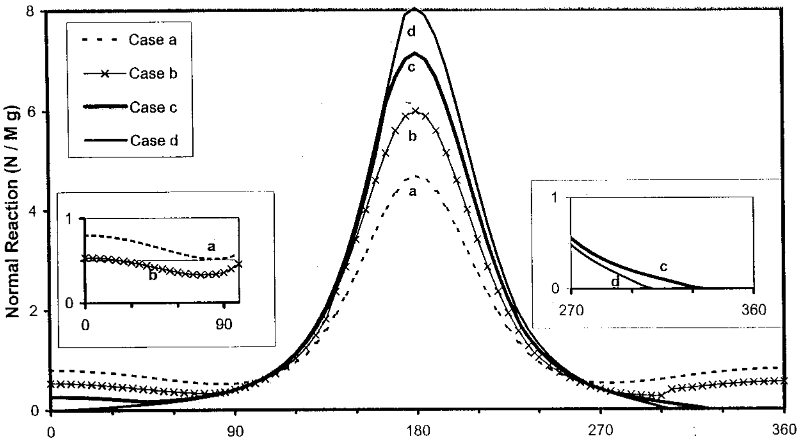

Fig. 3. Normal reaction as a function of position.

the acceleration due to gravity even though gravity is the only applied force. This aspect is discussed again later.

B. Initial position

In the initial position with $\theta=0$, the expressions for the reactions simplify to

$$F(0)=-0.5Mg(1-\gamma)\sin\varphi, \quad N(0)=Mg\gamma(\hat{\eta}_0-\eta_0), \tag{22}$$

after using (6), (14), and (15) in (13) and (10).

For rolling to take place in the initial position, it is necessary that the normal reaction is positive. This places an upper bound on the initial velocity, as the second equation of (22) implies that $N(0)>0$ requires that $\eta_0<\hat{\eta}_0$. If $\eta_0<\hat{\eta}_0$ the wheel will start rolling in the initial position provided that $\mu\geqslant|F(0)|/N(0)$, or, using (22),

$$\mu\geqslant\hat{\mu}=0.5(1-\gamma)\sin\varphi/\gamma(\hat{\eta}_0-\eta_0). \tag{23}$$

Here $\hat{\mu}$ denotes the *critical friction coefficient*; in the special cases of $\gamma=1$ or $\varphi=0$ this value is zero.

If $\eta_0\geqslant\hat{\eta}_0$, then $N(0)=0$, so that $\theta_*=0$ and $\eta_*=\eta_0$. Using (21) it follows that, if $\eta_0>\hat{\eta}_0$, the wheel hops immediately at $\theta=0$, due to the centrifugal effects of the large initial angular velocity. The range of values where this happens is shown as region IV in Figs. 6–8, which are discussed later.

If, however, $\eta_0=\hat{\eta}_0$, $\ddot{Y}_*^+=0$ and the higher derivatives are required to establish whether the wheel hops or not. Further differentiation of (20), simplified for $\ddot{\theta}=0$, results in $\dddot{Y}=g\gamma(-\dot{\theta}\eta\sin\theta)$; $\ddddot{Y}=(g^2/R)\gamma(-\eta^2\cos\theta)$. At point $\theta=0$ therefore, $\dddot{Y}_*^+=0$ and $\ddddot{Y}_*^+<0$. Because $\dot{Y}(0)=0$, this implies $Y(t)<R$, which is a contradiction; therefore (20) does not apply and the wheel cannot hop in this case, but starts skidding immediately. An example is shown as case d in the graphs in later sections.

C. The normal reaction on a horizontal plane

In the special case of a horizontal plane, the equations are readily analyzed and yield a number of interesting results. During the first rolling phase $\eta=(C_0-\gamma\cos\theta)/(1+\gamma\cos\theta)$, $\eta+1=(C_0+1)/(1+\gamma\cos\theta)$, $\zeta=0.5\gamma(\eta+1)\sin\theta/(1+\gamma\cos\theta)$, $F/Mg=0.5\gamma(\eta-1)\sin\theta$, and

$$N/Mg=0.5\delta^3/(1+\gamma\cos\theta)^2 + (1+\gamma\cos\theta)-0.5(1+C_0), \tag{24}$$

where $\delta^3=(1-\gamma^2)(1+C_0)=(1-\gamma)(1+\gamma)^2(1+\eta_0)$.

The first derivative of N can be written as

$$N'/Mg=\gamma\sin\theta(\delta^3(1+\gamma\cos\theta)^{-3}-1).$$

Setting this derivative equal to zero, the position θ_1 of a local extremum is found from $(1+\gamma\cos\theta_1)=\delta$, with the value $N_1=N(\theta_1)=0.5Mg(3\delta-(1+C_0))$.

The second derivative at this position is $N''(\theta_1)=3Mg\delta^{-1}\gamma^2\sin^2\theta_1$, which is clearly positive, indicating that this is in fact a minimum value.

For small enough values of γ and η_0, this local minimum is positive and, provided that μ is large enough, rolling continues through 360°. This situation corresponds to points in region I in Figs. 6–8, to be discussed later.

An example of this situation is shown as case a in Figs. 3–5, for the case $\mathcal{P}_0=\{0.5;0.3;0.6\}$. Using these values in the above relationships results in $\theta_1=84.5°$ and $N_1=0.51Mg$, which corresponds to the minimum point on the graph in Fig. 3, best seen on the insert showing the region $\theta=0-90$. The graph of F/N for case a in Fig. 4 shows that the rolling motion continues for the full rotation, reaching a maximum absolute value of 0.385. This hoop will therefore never slip if the friction coefficient exceeds this value.

Increasing γ and/or η_0 reduces this minimum value, and in many cases this value is negative, implying that N becomes zero at some point $\theta<\theta_1$. However, slipping will always occur before this point is reached, as illustrated by cases b–e below.

D. Examples of loaded hoops on a horizontal plane

The reaction forces are the main indicators of the types of motion when comparing the behavior of different cases. A number of examples are shown in Figs. 3–5. One result clearly seen on all these graphs is that N begins increasing immediately after slipping starts the first time, and that the normal reaction never becomes zero in a position $\theta<\pi$. Therefore the hoop cannot hop at a position $0<\theta<\pi$.

Case a shows the situation already discussed, where the minimum value of N is positive and the friction coefficient is large enough to ensure rolling through a full 360°. Note the

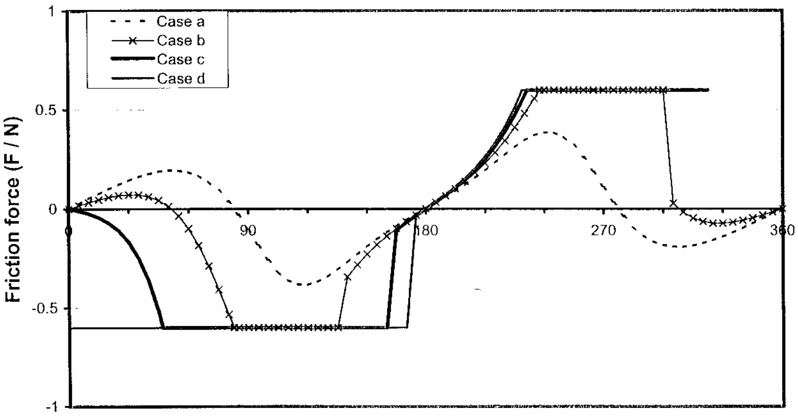

Fig. 4. F/N ratio as a function of position.

symmetry of the graphs of N and η about the point $\theta=\pi$, as could be expected for the conservative motion and also from (24).

In case b with $\mathcal{P}_0=\{0.5;0.7;0.6\}$, the increase in the initial velocity to $\eta_0=0.7$ causes a reduction in N due to the centrifugal effects so that the hoop starts skidding at position $\theta_2=82.7°$ as shown in Fig. 4, and the subsequent motion corresponds to that of case c as described previously, except that it does not bounce but ends with a final rolling phase.

When comparing cases b and c, it is clear that increasing the value of the initial velocity has the effect of reducing the angle where rolling stops and that the skidding phase continues over a larger region. This aspect reaches a limit when the initial velocity equals the critical value $\hat{\eta}_0$. In this case, shown as case d with $\mathcal{P}_0=\{0.5;1.5;0.6\}$, $N=0$ at $\theta=0$ and skidding starts immediately, continuing until just before 180°, where a short rolling phase starts, followed by spinning before hopping at $\theta_*=303.4°$. The positions where N becomes zero in cases c and d are clearly seen in the inset in Fig. 3 showing the region 270°–360°.

Graphs of the angular velocity are shown in Fig. 5. In all cases the graph peaks at 180°. The graph of case a is symmetrical because it is a conservative motion and the angular velocity after one revolution again reaches the initial value. In contrast, case b ends with $\eta=0.692$, a value slightly less than the initial value due to the loss of energy during the skidding and spinning phases. In case c the graph ends when the hoop bounces with a reasonably large angular velocity as required by (21).

The graph for case e, with $\mathcal{P}_0=\{0.03;0.1;0.6\}$, illustrates another possibility. This case is similar to b, except that the very small mass ratio and low initial velocity plus loss of energy due to friction results in the motion stopping before reaching $\theta=2\pi$. This is clearly shown in Fig. 5 where $\eta=0$ at position $\theta=335°$.

Finally, the insert in Fig. 5 showing case f illustrates the effect of the slope. Here $\mathcal{P}=\{0.5;0.0;0.6;10\}$ was used, having the same general characteristics as case a. However, because of the 10° slope the final angular velocity is much greater than the initial value, which was taken as zero for this example. The calculated value of $\eta(2\pi)=0.6546$ corresponds exactly to the theoretical value of $2\pi\sin\varphi/(1+\gamma)$, which is obtained by equating the gain in kinetic energy to the loss of potential energy. The kinetic energy at position $\theta=2\pi$ is $E_k=0.5I_c\dot{\theta}^2=MgR(1+\gamma)\eta$, taking rotation about point of contact C; the loss in potential energy after one revolution is $E_g=Mg2\pi R\sin\varphi$, as seen from Fig. 1.

E. Regions on the $\eta_0-\nu$ plane

The previous results can be clearly summarized by identifying five different regions on the $\nu-\eta_0$ plane (for specific

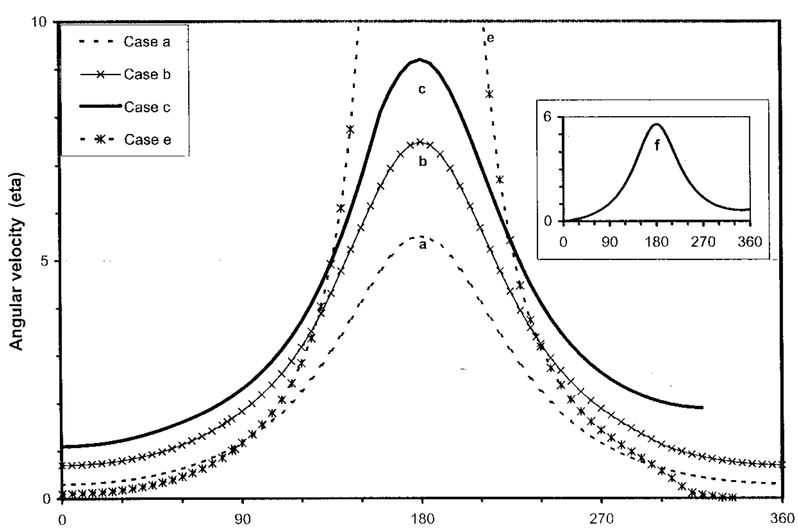

Fig. 5. Angular velocity η as a function of position.

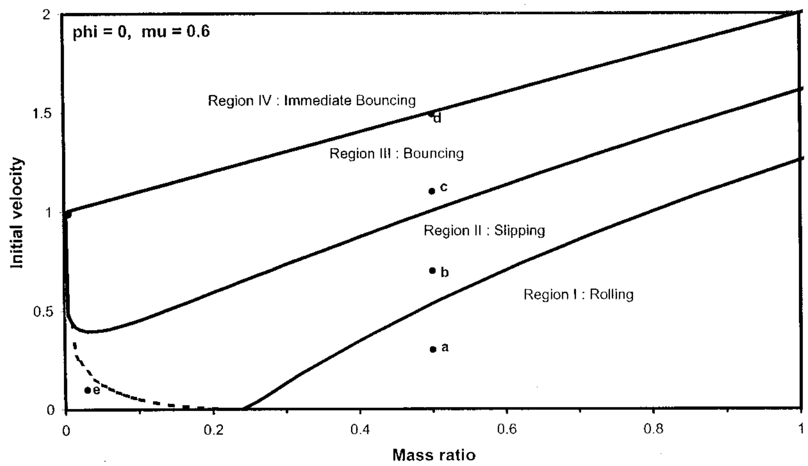

Fig. 6. Different regions on the $\eta_0 - \nu$ plane.

values of φ and μ). Figure 6 was drawn for the case $\varphi = 0$ and $\mu = 0.6$, with points a–e indicating the examples discussed previously.

Points in the lowest region, shown as region I, correspond to those cases where rolling will occur through the full 360° without slipping, as shown in case a. This is of course a conservative motion, with no loss of energy.

Points in region II correspond to those cases where slipping begins at a position $\theta \leqslant \pi/2$, as illustrated by cases b and e. Region II contains a small subregion near the origin. Hoops starting with parameters in this region, such as case e, do not have sufficient initial kinetic energy to complete a full revolution, and come to a standstill before the particle reaches the highest point again.

Region III contains the interesting cases where the hoop will bounce at a position where the particle is moving upwards, such as cases c and d. The high initial angular velocity in region IV causes the hoop to bounce immediately at $\theta = 0$ as previously discussed.

The line separating regions I and II was found by numerical experimentation with the computer program, and shows the largest initial velocity for which the hoop will continue rolling without slipping. The line separating regions II and III was found in a similar manner and shows the smallest initial velocity for which the hoop will bounce. The line separating regions III and IV represents the line $\eta_0 = \hat{\eta}_0$, as given by (6).

F. Influence of the friction coefficient and the slope

The effect of different values of μ and φ can be shown clearly by comparing the four regions on the $\nu - \eta_0$ plane for different cases.

Figure 7 shows the regions for a horizontal plane where μ has been halved to 0.3. The regions for the previous case of $\mu = 0.6$ are shown as dotted lines. A reduction in μ has the effect of reducing region I and increasing regions II and III, with slipping starting at a lower initial velocity as could be expected.

An increase in the slope has a similar effect, as shown in Fig. 8, where μ is kept at 0.6 but $\varphi = 10°$. In this case the increase in kinetic energy as the hoop rolls down the slope makes it ''easier'' to hop and region III is much larger than the corresponding region for the horizontal plane. The position of case f is seen to be inside region I, which is in agreement with the earlier analysis.

These aspects will not be investigated further; let it suffice to point out that for a given friction coefficient an upper limit for the slope is defined by (23), which can be rewritten in the form $\sin \varphi \leqslant 2\mu(\cos \varphi - \gamma\eta_0)/(1-\gamma)$. This simplifies to $\tan \varphi \leqslant 2\mu/(1-\gamma)$ for the case $\eta_0 = 0$. If this is exceeded, the wheel cannot roll initially, but slips from the start.

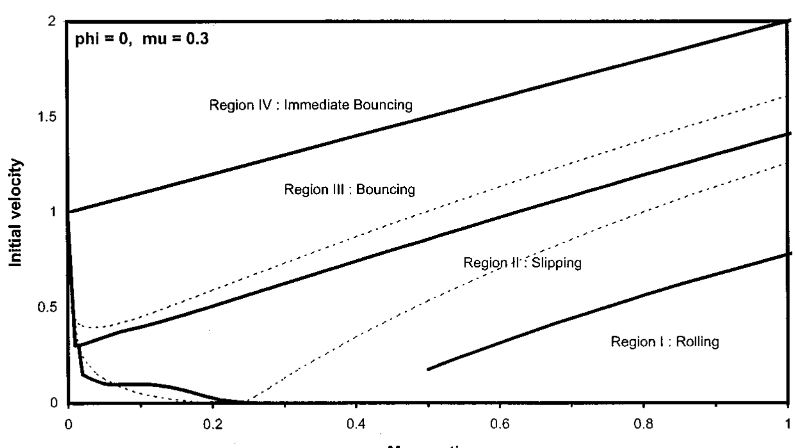

Fig. 7. Influence of the friction coefficient μ.

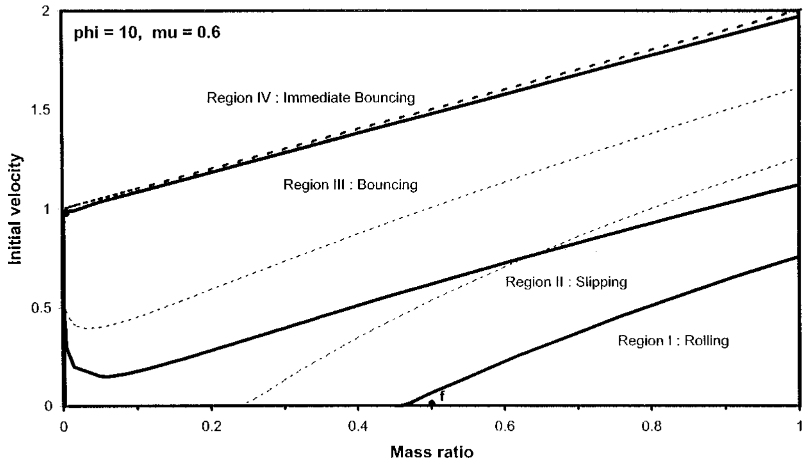

Fig. 8. Influence of the slope φ.

G. Accelerations exceeding *g*

Another interesting facet of a loaded wheel with large eccentricity is that extremely large accelerations occur in the vicinity of $\theta=\pi$, as already noticed in Fig. 2. This phenomenon can be explained by noting that the moment of inertia about the contact point C is extremely small in this position in cases where $\gamma\rightarrow 1$. For example, in the case of a hoop and $\theta=\pi$, $\kappa_C=2(1-\gamma)$ from (1). Division by this small value in Eqs. (14) and (15) for rolling leads to very large velocities and accelerations.

This aspect can be analyzed in cases where the hoop rolls through position $\theta=\pi$ on a horizontal plane. Using (7) and (8), the nondimensional acceleration of the center of gravity can be written as

$$a^2=\gamma^2\eta^2+(\gamma^2+1+2\gamma\cos\theta)\zeta^2-2\gamma\eta\zeta\sin\theta.$$

Differentiating with respect to θ and using $\eta'=2\zeta$ results in

$$2aa'=2\gamma\zeta(2\gamma\eta-\eta\cos\theta-3\zeta\sin\theta \\ +\zeta'(2\cos\theta+\gamma+\gamma^{-1}))-2\gamma\eta\zeta'\sin\theta.$$

Also, using $\varphi=0$ in (14) and (15), $\zeta=2\gamma(C+1)\sin\theta/\kappa_C^2$. At position $\theta=\pi$ therefore, $\kappa_C=2(1-\gamma)$, $\zeta=0$, $\eta'=0$, and $a'=0$. Therefore both η and a reach local extrema at this point, denoted by η^* and a^*, respectively; the graphs clearly show that these are maximum values.

Using $\theta=\pi$ in (15), (7), and (8), $\eta^*=(C+\gamma)/(1-\gamma)$, $\ddot{x}=0$, $\ddot{y}/g=\gamma\eta^*$, and $a^*=\gamma\eta^*$.

For cases in region I, $C=C_0=\eta_0(1+\gamma)+\gamma\cos\varphi$, and case a for example with $\gamma=2/3$ and $\eta_0=0.3$ results in $C_0=7/6$, $\eta^*=11/2$ and $a^*=11/3$. The value of η^* is confirmed by Fig. 5.

As a second example, the equal mass case with zero initial velocity, $\mathcal{P}_0=\{1.0;0.0;0.6\}$, at the bottom right-hand corner in Fig. 6, gives $C_0=\gamma=0.5$, $\eta^*=2$, and $a^*=1$. The computer calculations show that a minimum value of $\mu=0.204$ is required to prevent slipping in this case.

All other cases corresponding to points in Fig. 6 have values $a^*>1$, as can be seen in Fig. 9, which shows some lines of constant a^* (or contours of a^*) on the $\nu-\eta_0$ plane. In all these cases therefore the acceleration of point G is greater than g.

The above analysis is in agreement with the graphs given previously, and also explains the extremely large peak values, in, for example, case e where $\nu=0.03$ or $\gamma=0.971$ represents a very large eccentricity and values of $\eta^*=64$ and $a^*=62.1$ are calculated at 180°. These calculated values are in agreement with the relationship found above that $a^*=\gamma\eta^*$.

As $\nu\rightarrow 0$, i.e., $\gamma\rightarrow 1$ and $\kappa_C\rightarrow 0$, these values tend to infinity. The present implementation of the algorithm gave values of $a^*=223$ for $\nu=0.01$, and $a^*>10^3$ for $\nu=0.001$. However, the algorithm becomes unstable for $\theta>\pi$ with such very small values of ν.

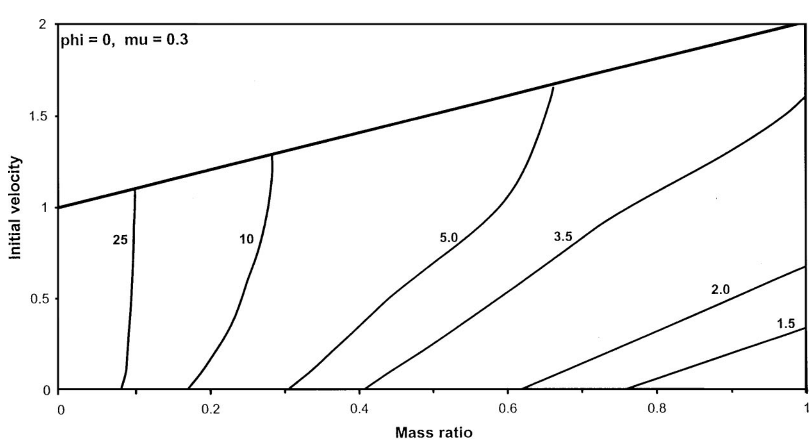

Fig. 9. Lines of constant a^*, the maximum acceleration of G.

H. Massless hoops

We now return to the original problem of the massless hoop rolling on a horizontal plane, and consider it in the context of the solutions developed in this paper. Now $\gamma = 1$, $\kappa_C = 2(1+\cos\theta)$ and, very significantly, $I_G = 0$. Therefore Newton's second law requires that the torque around G always be zero, but provides no information whatsoever about $\ddot{\theta}$.[8]

The previous solution for rolling motion also applies for the massless case, so that (13)–(15) and (24) simplify to $C_0 = 1 + 2\eta_0$, $\eta = 2(C_0 - \cos\theta)/\kappa_c$, $\zeta = (\eta+1)\sin\theta/\kappa_c$, $F/Mg = (1+\cos\theta)\zeta - \eta\sin\theta$, and

$$N/Mg = \cos\theta - \eta_0 .$$

From these equations, $F/N = \tan(\theta/2)$, thus satisfying the requirement of zero torque around G.

In Littlewood's original problem $\eta_0 = 0$ so that the normal reaction becomes zero at $\theta_* = \pi/2$, with $\eta_* = 1$ and $\zeta(t_*^-) = 1$, where the negative sign $(-)$ denotes the possibility of a discontinuity in the angular acceleration.

The requirement for zero torque implies that the reaction remains zero for $\theta > \theta_*$, in which case $\ddot{y} = -g$ and the particle's path changes from a cycloid to a parabola.[1] However, none of the above necessarily implies "hopping."

As before, a sufficient condition for any rigid hoop to hop is that $\ddot{Y}(t_*^+) > 0$. In the case under consideration, (7) results in $\ddot{Y}(t_*)/g = -1 + \zeta(t_*)$. Therefore, the hoop will hop as suggested by Littlewood and Tokieda only if there is a discontinuous increase in the angular acceleration from $\ddot{\theta}(t_*^-) = g/R$ to $\ddot{\theta}(t_*^+) > g/R$.

In Ref. 5 we show that an alternative motion exists in which there is no discontinuity in the angular acceleration. In this rather strange motion which we call "*skimming*" the particle follows a parabolic path while the center of the hoop continues moving horizontally so that the hoop maintains contact with the surface even though the reaction on the hoop remains zero. This is a conservative motion (because of zero friction), which ends at position $\theta = \pi$ where the solution becomes indeterminate and the particle collides with the surface.

The motion of loaded massless hoops is considered in detail in a separate paper,[5] where the influence of nonzero initial velocities and the effect of friction is also analyzed.

Finally, it is also of some interest to note that Butler's proof[2] that Littlewood's hoop does not hop is based on the assumption that $\ddot{\theta}(t_*^+) = 0$. This assumption, based on the argument that this would be the case for real hoops with (infinitely small) mass, was also used erroneously in earlier versions of this paper. However, as shown above, this does not apply for massless hoops.[8]

IV. CONCLUSIONS

The main results of the analysis of real, rigid hoops loaded with heavy particles and rolling on a rough horizontal surface can be summarized as follows.

(a) The hoop will hop after rotating through more than 270°, provided the initial velocity is large enough to be in region III, as shown in Figs. 6–8.

The hoop will hop immediately if the initial velocity exceeds the critical value $\hat{\eta}_0$ defined in (6).

(b) In all cases where the mass of the particle exceeds that of the hoop, the acceleration of the center of mass will be greater than g when the particle is close to the lowest point of its trajectory.

(c) The effect of different initial velocities is clearly illustrated by cases a–d, where η_0 was the only parameter to be changed.

In the hypothetical case of Littlewood's massless hoop, it is shown that the hoop does not necessarily hop but that an alternative motion called skimming is possible.

Note added in proof. A recent paper by Pritchett[9] came to my attention just after this paper was accepted for publication. Pritchett's model is virtually the same as the model analyzed above, except that Pritchett's hoop is loaded with a "particle" with finite dimensions. Therefore $I_G > 0$ even when the hoop is massless, allowing Pritchett to use $\ddot{\theta}(t_*^+) = 0$ in order to prove that a hoop (real or massless) cannot hop if the "no slipping" condition is adhered to. This is in agreement with our results. However, Pritchett claims that hopping is possible when $\theta \approx \pi/2$. He includes a photograph showing a loaded hula hoop hopping, which phenomenon we are inclined to attribute to the elasticity of the hoop. More seriously, he includes a corresponding graphical representation of a numerical simulation of a real hoop, with the hop occurring at approximately $\theta = \pi/2$. This is in direct contradiction with our results; at this stage the only explanation seems to be the different numerical methods used once the hoop starts slipping. Our results, for example, Fig. 2, show that the normal reaction starts *increasing* at the onset of slipping. We remain convinced that a *rigid* hoop cannot hop when $\theta \approx \pi/2$.

[a]Electronic mail: wfdt@maties.sun.ac.za

[1]T. F. Tokieda, "The Hopping Hoop," Am. Math. Monthly **104**, 152–153 (1997).
[2]J. P. Butler, "Hopping Hoops Don't Hop," Am. Math. Monthly **106**, 565–568 (1999).
[3]J. E. Littlewood, *Littlewood's Miscellany* (Cambridge U.P., Cambridge, 1986).
[4]W. F. D. Theron and N. M. du Plessis, "The hopping hoop revisited," Departmental Report TW98/1, Department of Applied Mathematics, University of Stellenbosch, Stellenbosch, 1998.
[5]W. F. D. Theron and N. M. du Plessis, "The dynamics of a massless hoop" (unpublished).
[6]W. F. D. Theron, "Bouncing due to the 'infinite jerk' at the end of a circular track," Am. J. Phys. **63**, 950–955 (1995).
[7]W. F. D. Theron, "The 'faster than gravity' demonstration revisited," Am. J. Phys. **56**, 736–739 (1988).
[8]The author gratefully acknowledges these insights provided by M. S. Tiersten, a reviewer of the original paper.
[9]T. Pritchett, "The Hopping Hoop Revisited," Am. Math. Monthly **106**, 609–617 (1999).